Clinical Chemistry 49:3
396–406 (2003)

Amplicon Melting Analysis with Labeled Primers: A Closed-Tube Method for Differentiating Homozygotes and Heterozygotes

Cameron N. Gundry, Joshua G. Vandersteen, Gudrun H. Reed, Robert J. Pryor, Jian Chen, and Carl T. Wittwer*

Background: **Common methods for identification of DNA sequence variants use gel electrophoresis or column separation after PCR.**

Methods: **We developed a method for sequence variant analysis requiring only PCR and amplicon melting analysis. One of the PCR primers was fluorescently labeled. After PCR, the melting transition of the amplicon was monitored by high-resolution melting analysis. Different homozygotes were distinguished by amplicon melting temperature (T_m). Heterozygotes were identified by low-temperature melting of heteroduplexes, which broadened the overall melting transition. In both cases, melting analysis required ~1 min and no sample processing was needed after PCR.**

Results: **Polymorphisms in the *HTR2A* (T102C), β-globin [hemoglobin (Hb) S, C, and E], and cystic fibrosis (F508del, F508C, I507del, I506V) genes were analyzed. Heteroduplexes produced by amplification of heterozygous DNA were best detected by rapid cooling (>2 °C/s) of denatured products, followed by rapid heating during melting analysis (0.2–0.4 °C/s). Heterozygotes were distinguished from homozygotes by a broader melting transition, and each heterozygote had a uniquely shaped fluorescent melting curve. All homozygotes tested were distinguished from each other, including Hb AA and Hb SS, which differed in T_m by <0.2 °C. The amplicons varied in length from 44 to 304 bp. In place of one labeled and one unlabeled primer, a generic fluorescent oligonucleotide could be used if a 5′ tail of identical sequence was added to one of the two unlabeled primers.**

Conclusion: **High-resolution melting analysis of PCR products amplified with labeled primers can identify both heterozygous and homozygous sequence variants.**

There are many methods for identifying sequence variants. Single-nucleotide polymorphism typing is perhaps the simplest case, where the expected result is limited to only one of two bases at a given position. If sequence variation occurs at more than one position but is limited to a small region, a probe placed over the region of interest can be used to detect variants. Unique variants can often be distinguished by differences in the probe melting temperature (T_m)[1] *(1)*, a homogeneous procedure that can be automatically performed after PCR in a closed-tube system.

When an entire PCR product needs to be monitored for variation, gel electrophoresis or column separation after PCR is usually required. Monitoring methods include single-strand conformation polymorphism *(2)*, heteroduplex migration *(3)*, denaturing gradient gel electrophoresis *(4)*, temperature gradient gel electrophoresis *(5)*, and enzyme or chemical cleavage methods *(6)*. Sequencing also requires multiple steps after PCR, namely cycle sequencing and gel electrophoresis. Denaturing HPLC *(7)* does not require gels; instead, a sample of the PCR product is injected into a column. Although some of these methods can be automated, a procedure for mutation analysis that would not require PCR product separation on gels or columns would simplify the process.

SYBR Green I is a double-strand-specific DNA dye often used to monitor product formation *(8)* and T_m *(9)* in real-time PCR. The presence of heterozygous single base changes has been detected in products up to 167 bp by

Department of Pathology, University of Utah Medical School, Salt Lake City, UT 84132.
*Author for correspondence.
Received September 27, 2002; accepted December 5, 2002.

[1] Nonstandard abbreviations: T_m, melting temperature; HTR2A, hydroxytryptamine receptor 2A; and Hb, hemoglobin

melting curve analysis with SYBR Green I *(10)*. However, between PCR and melting analysis, the PCR product was purified and high concentrations of SYBR Green I were added. The concentration of SYBR Green I used inhibits PCR *(8)*, so the dye was added after amplification. In another report, SYBR Green I melting analysis was used to detect heterozygous single-nucleotide polymorphisms in products up to 212 bp *(11)*. However, a GC clamp on one primer and adjustment of the solution to 12 mol/L urea before melting curve generation were necessary. In both cases, the addition of reagents after PCR was required. Any manipulation of the sample increases the risk of PCR product carryover into subsequent reactions.

Another option for homogeneous amplicon analysis is the use of multiple hybridization probes, each labeled with a fluorescent dye *(8, 12)*. Such probes have been tiled across amplicons to scan for p53 mutations *(13)*. Although this method is truly single step and requires no additions, the need for multiple probes to cover all potential mutation sites limits its usefulness.

We recently noted a change in fluorescence when 5′-labeled oligonucleotides were hybridized *(14)*. In this report, we demonstrate that use of a 5′-labeled primer enables melting profiles of the amplicon to be obtained immediately after PCR. Melting curve analysis allows identification of sequence variants without additions, purification, or separation of PCR products. Furthermore, high-resolution melting curve analysis produces different shapes for different heterozygotes, often allowing identification of the specific sequence variant. Similarly, different homozygotes can often be distinguished, including homozygotes that differ by only a single base. We focus on demonstrating the technique by genotyping known sequence variants. We also discuss the potential of the method for detecting unknown variants (so-called "mutation scanning").

Materials and Methods

PCR PROTOCOL

Labeled and unlabeled oligonucleotides were obtained from IT Biochem, Qiagen Operon, or Synthegen. Purity was assessed by absorbance as described previously *(12)*. PCR was performed in 10-μL volumes in a LightCycler (Roche Applied Systems) with programmed transitions of 20 °C/s unless otherwise indicated. The amplification mixture included 50 ng of genomic DNA as template, 200 μM each deoxynucleotide triphosphate, 0.4 U of KlenTaq1 polymerase (AB Peptides), 88 ng of TaqStart antibody (ClonTech), 3 mM $MgCl_2$, 50 mM Tris (pH 8.3), 500 μg/mL bovine serum albumin, and 0.5 μM primers unless otherwise indicated. Genotyped human genomic DNA was obtained from previous studies *(15, 16)* or from Coriell Cell Repositories. The DNA used for β-globin genotyping was extracted from dried blood spots *(17)*. When SYBR Green I was used as the indicator instead of labeled primers, a 1:30 000 final dilution from the Molecular Probes stock was used.

MELTING CURVE ACQUISITION

Melting analysis was performed either on the LightCycler immediately after cycling or on a high-resolution melting instrument (HR-1; Idaho Technology). For high-resolution melting, the sample was first amplified in the LightCycler and then heated momentarily in the LightCycler to 94 °C and rapidly cooled (program setting of −20 °C/s) to 40 °C unless otherwise stated. The LightCycler capillary was then transferred to the high-resolution instrument and heated at 0.3 °C/s unless otherwise stated. The HR-1 is a single-sample instrument that surrounds one LightCycler capillary with an aluminum cylinder. The system is heated by Joule heating through a coil wound around the outside of the cylinder. Sample temperature is monitored with a thermocouple, also placed within the cylinder, and converted to a 16-bit digital signal. Fluorescence is monitored by epi-illumination of the capillary tip *(18)*, which is positioned at the bottom of the cylinder, and also converted to a 16-bit signal. Approximately 50 data points are acquired for every 1 °C.

MELTING CURVE ANALYSIS

LightCycler and high-resolution melting data were analyzed with custom software written in LabView (National Instruments). Fluorescence-vs-temperature plots were normalized between 0% and 100% by first defining linear baselines before and after the melting transition of each sample. Within each sample, the fluorescence of each acquisition was calculated as the percentage fluorescence between the top and bottom baselines at the acquisition temperature. In some cases, derivative melting curve plots were calculated from the Savitsky–Golay polynomials at each point *(19)*. Savitsky–Golay analysis used a second-degree polynomial and a data window including all points within a 1 °C interval. Peak areas and T_ms were obtained by nonlinear least-squares regression to fit multiple Gaussians.

GENOTYPING AT THE CYSTIC FIBROSIS GENE (M55115) WITH LABELED PRIMERS OR SYBR GREEN I

A 44-bp fragment was amplified with the primers 5′-GGCACCATTAAAGAAAATAT-3′ (position 413) and 5′-TCATCATAGGAAACACCA-3′ (position 456R). The first primer was 5′-labeled with Oregon Green 91, or SYBR Green I was included in the reaction. The primers flank the mutational hot spot containing the F508del, I507del, and F508C variants. PCR was performed through 40 cycles of 85 and 58 °C (0 s holds). A final melting cycle was performed on the LightCycler by heating to 95 °C, cooling to 55 °C, and then collecting fluorescence continuously at a ramping rate of 0.2 °C/s. Six samples were monitored during melting curve acquisition.

EFFECT OF COOLING RATE, HEATING RATE, AND Mg^{2+} CONCENTRATION ON HETERODUPLEX DETECTION

Using the 44-bp cystic fibrosis amplicon, we studied the effects of cooling rate, heating rate, and Mg^{2+} concentra-

tion on heterozygous F508del DNA on the LightCycler. To study the effect of cooling rate, the samples were amplified, heated to 85 °C, and then cooled from 85 to 60 °C at 20, 5, 2, 1, 0.5, 0.1, or 0.05 °C/s, followed by a constant heating rate of 0.2 °C/s for melting curve acquisition. The effect of heating rate was studied by cooling at 20 °C/s, followed by melting at 0.05, 0.1, 0.2, or 0.4 °C/s. The effect of cations (Mg^{2+} concentration) was studied by adjusting the concentration of the amplicon after PCR with $MgCl_2$ to 1, 2, 3, 4, or 5 mM, keeping all other concentrations constant (e.g., amplicon, buffer).

HTR2A (NM_000621) single-nucleotide polymorphism

Three primer sets flanked the common polymorphism (T102C) within exon 1 of the hydroxytryptamine receptor 2A (*HTR2A*) gene *(10)*. A 115-bp fragment was amplified with forward primer 5′-CACCAGGCTCTACAGTAATG-3′ (217) and reverse primer 5′-TGAGAGGCACCCTTCACAG-3′ (331R). In addition, 152- and 304-bp fragments were amplified with forward primer 5′-GCTCAACTACGAACTCCCT-3′ (180) and reverse primers 5′-TGAGAGGCACCCTTCACAG-3′ (331R) and 5′-AGGAAATAGTTGGTGGCATTC-3′ (483R), respectively. The forward primers were 5′-labeled with 6-carboxyfluorescein. The polymorphism was 30 bases from the labeled end of the 115-bp product and 67 bp away from the labeled ends of the 152- and 304-bp products. The 115- and 152-bp reactions were cycled 40 times between 95 °C with no hold, 65 °C with a 1 s hold, and 74 °C with a 10 s hold. The 304-bp reaction was cycled 40 times between 95 °C with no hold, 62 °C with a 2 s hold, and 74 °C with a 20 s hold. A high-resolution melting curve was obtained.

β-globin mutations (hemoglobin S, C, and E)

A 113-bp fragment of the β-globin gene (GI: 455025) was amplified with primers Oregon Green-TGCACCTGACTCCT-3′ (62191) and 5′-CCTGTCTTGTAACCTTG-3′ (62303R). The primers flank three single-nucleotide polymorphisms: hemoglobin (Hb) C (G16A), Hb S, (A17T), and Hb E (G76A). For the homozygote study (Fig. 6), standard Oregon Green labeling was used. The samples were cycled 37 times through the following protocol: 94 °C with no hold, 55 °C with no hold, and a 2 °C/s ramp to 72 °C with a 2 s hold. For all other studies at the β-globin locus (Figs. 5, 7, and 8), Oregon Green labeling used SimpleProbe™ chemistry (Idaho Technology). When SimpleProbe chemistry was used, PCR was performed in 100 mM 2-amino-2-methyl-1,3-propanediol, pH 8.8, with 0.04 U/μL *Taq* polymerase (Roche). After an initial denaturation for 10 s at 95 °C, the samples were cycled 45 times with the following protocol: 95 °C with no hold, 51 °C with a 6 s hold, and a 1 °C/s ramp to 72 °C with no hold.

Generic indicator primer. The use of a generic indicator primer to detect polymorphisms was demonstrated using cystic fibrosis polymorphisms. In place of a locus-specific labeled primer, an unlabeled primer with a 5′ tail not homologous to the target was used. This 5′ tail is identical in sequence (without the 5′ G) to a generic indicator primer that is fluorescently labeled and also present in the reaction. Different loci can be studied with the same generic primer by simply adding the unlabeled 5′ sequence tail to one of the locus-specific primers *(20)*. A 243-bp fragment (214-456R) was amplified with the primers 5′-AGAATATACACTTCTGCTTAG-3′ (0.5 μM) and 5′-GCTGCACGCTGAGGTTCATCATAGGAAACACCA-3′ (0.05 μM). The underlined sequence is the target-independent tail, identical in sequence (minus one G) to the generic indicator primer (6-carboxyfluorescein)-GGCTG-CACGCTGAGGT-3′ (0.5 μM). The indicator primer is similar, but not identical to, a previously used universal primer *(20)* and does not show significant homology to human sequences. The PCR was performed with 50 cycles between 86 °C (0 s hold), 57 °C (0 s hold), and 67 °C (20 s hold). After a final denaturation and rapid cooling, a high-resolution melting curve was obtained.

Results

Derivative melting curves of PCR products amplified from different genotypes at the I507/F508 region of the cystic fibrosis gene are shown in Fig. 1. The PCR products were 41 or 44 bases long (Fig. 1A). Either a 5′-labeled primer (Fig. 1B) or SYBR Green I (Fig. 1C) was used for fluorescent monitoring of the melting transition between double- and single-stranded products. Results from two homozygous and three heterozygous genotypes are shown. When only the major melting transition is considered, SYBR Green I (compared with labeled primers) increased the T_m by ~2 °C and reduced the temperature difference between genotypes. The mean (SD) T_m of all five genotypes with labeled primers was 70.74 (0.48) °C compared with 72.73 (0.37) °C with SYBR Green I. The duplex stabilities of the different genotypes followed theoretical calculations *(21)*, with F508del ~ I507del < wild type < F508C. Except for F508del and I507del, the genotypes are distinguishable by the T_ms of their major transitions. The SD of the T_m of 10 replicate wild-type samples was 0.12 °C when melted on the LightCycler. When melted on the high-resolution instrument, the SD of the T_m of the same 10 samples was 0.04 °C.

When a heterozygous sample is amplified by PCR, two homoduplex and two heteroduplex products are expected *(3)*. However, when SYBR Green I was used as the fluorescent indicator, only a single melting peak was apparent for each genotype (Fig. 1C). In contrast, when labeled primers were used under the same conditions, two clearly defined peaks appeared (Fig. 1B). The lower temperature peak was always smaller than the higher temperature peak and presumably indicates the melting transition of one or both heteroduplex products. As might be expected, the heterozygotes with 3 bp deleted (F508del and I507del) produced heteroduplex peaks that were more destabilized than heteroduplex peaks from a single base change (F508C). The primary peak from the F508C heterozygote was at a higher temperature than the wild

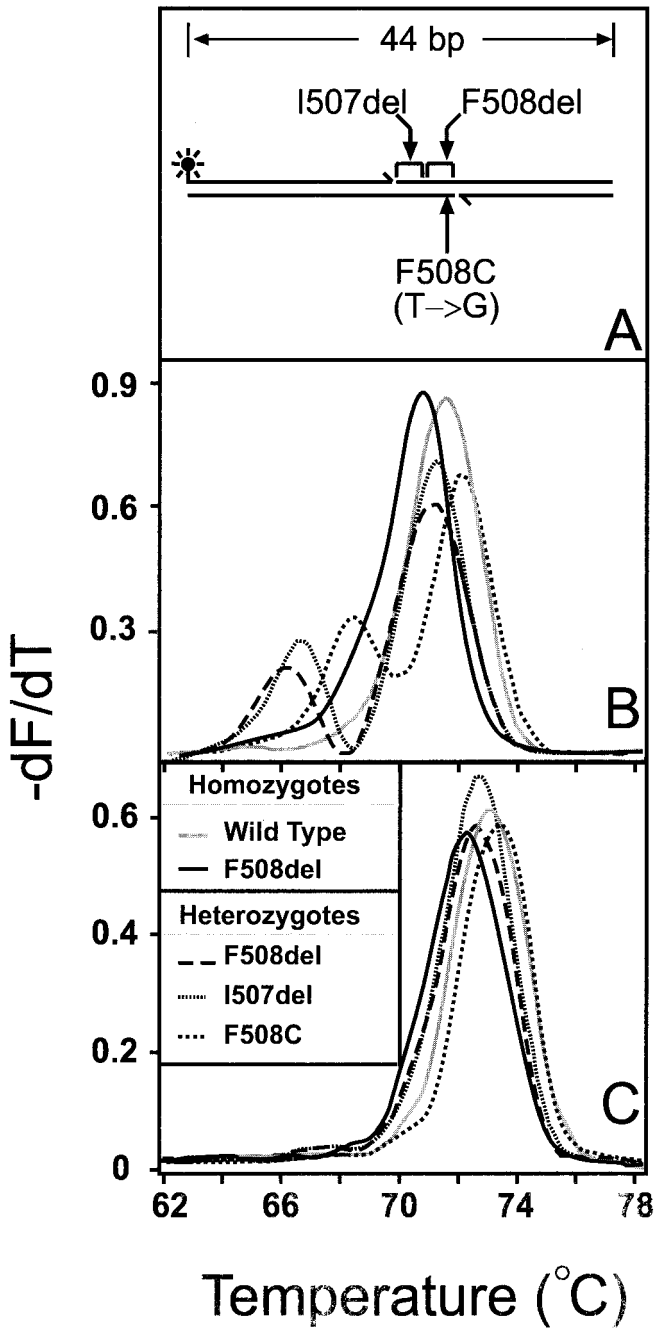

Fig. 1. Genotyping of the I507/F508 region of the cystic fibrosis gene using either a labeled primer or SYBR Green I.

(*A*), scaled drawing of the 44-bp amplicon. When a labeled primer is used (*B*), the derivative melting curves show clearly separated heteroduplex products that melt at lower temperatures than homoduplex products. Oregon Green was attached to a 5′ G residue in the primer, producing a 19% decrease in fluorescence during melting. When SYBR Green I is used (*C*) instead of a labeled primer, no heteroduplex peaks are apparent. In both cases, two homozygotes and three heterozygotes were studied. The LightCycler was used for melting curve acquisition.

type, reflecting the greater stability of the T-to-G transversion *(15)*.

For heteroduplexes to melt, they must first be formed from denatured heterozygous PCR products during cooling. The effect of heating and cooling rates on heteroduplex formation was studied with the F508del heterozygote and the 41-/44-bp amplicon. Under our conditions, rapid cooling was necessary for substantial heteroduplex formation (Fig. 2). Heteroduplexes were not observed when the cooling rate was <0.1 °C/s. The greatest heteroduplex formation occurred when capillary samples were rapidly transferred from boiling water to ice water (data not shown). With cooling on the LightCycler, heteroduplex formation appeared to plateau at programmed rates >5 °C/s (Fig. 2). However, measurement of actual sample temperatures showed that the cooling rate increased only slightly with programmed rates >5 °C/s.

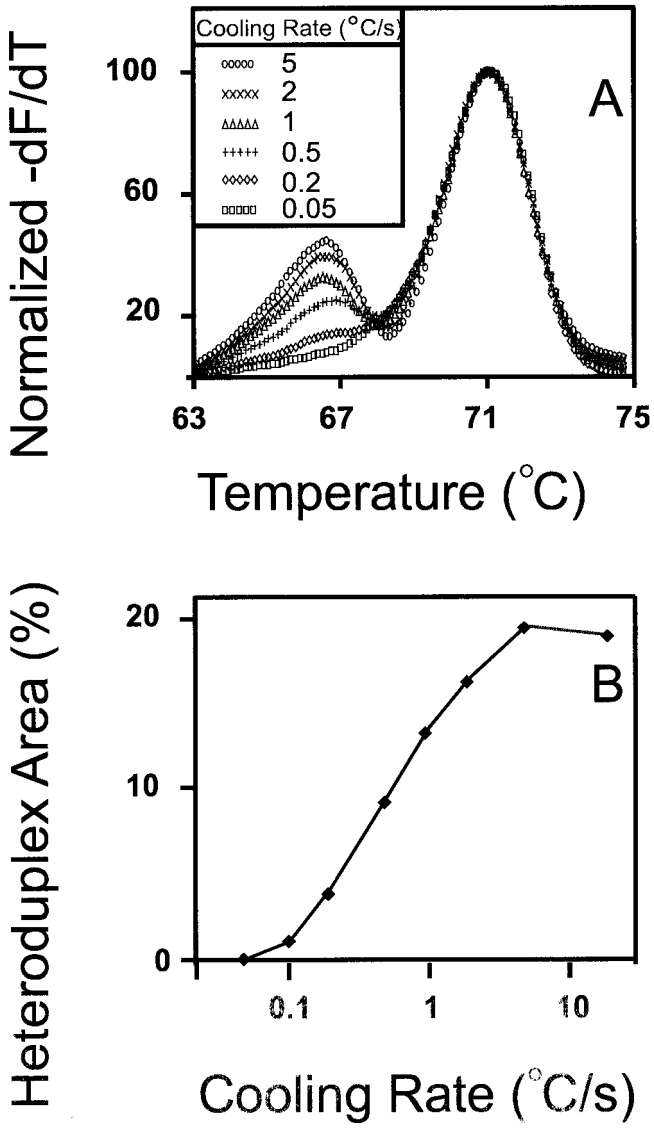

Fig. 2. Heteroduplex formation is greater with rapid cooling.

Heterozygous F508del DNA at the cystic fibrosis locus was amplified with one labeled primer as in Fig. 1B. The sample was repeatedly denatured, cooled at different programmed rates, and melted at 0.2 °C/s. Heteroduplex detection was greater at faster cooling rates. (*A*), derivative melting curves normalized to the homoduplex peak height. (*B*), heteroduplex peak area (%) plotted against cooling rate. The LightCycler was used for melting curve acquisition.

The relative percentage of heteroduplexes was greater with higher heating rates (Fig. 3). At 0.4 °C/s, the heteroduplex area was 30%, whereas at 0.05 °C/s, this area was ~10%. The apparent T_m also shifts to higher temperatures as the rate increases and the melting process deviates more from equilibrium *(15)*. In addition, very high rates limit the number of fluorescent acquisitions that can be obtained per temperature interval.

We also found that heteroduplex formation increased as the ionic strength decreased (data not shown). The greatest effect was observed with Mg^{2+}, although K^+ and $Tris^+$ also showed this effect to some extent. Under certain heating and cooling conditions, no heteroduplexes were observed at high Mg^{2+} concentrations (5 mM). However, as the Mg^{2+} concentration was reduced to 1 mM, the heteroduplex peak progressively increased. As expected, decreasing the ionic strength also decreased the T_m *(21)*. In all studies that follow, the cooling rate was set to maximum (programmed at 20 °C/s), the heating rate was 0.2–0.3 °C/s, and the high-resolution melting instrument was used.

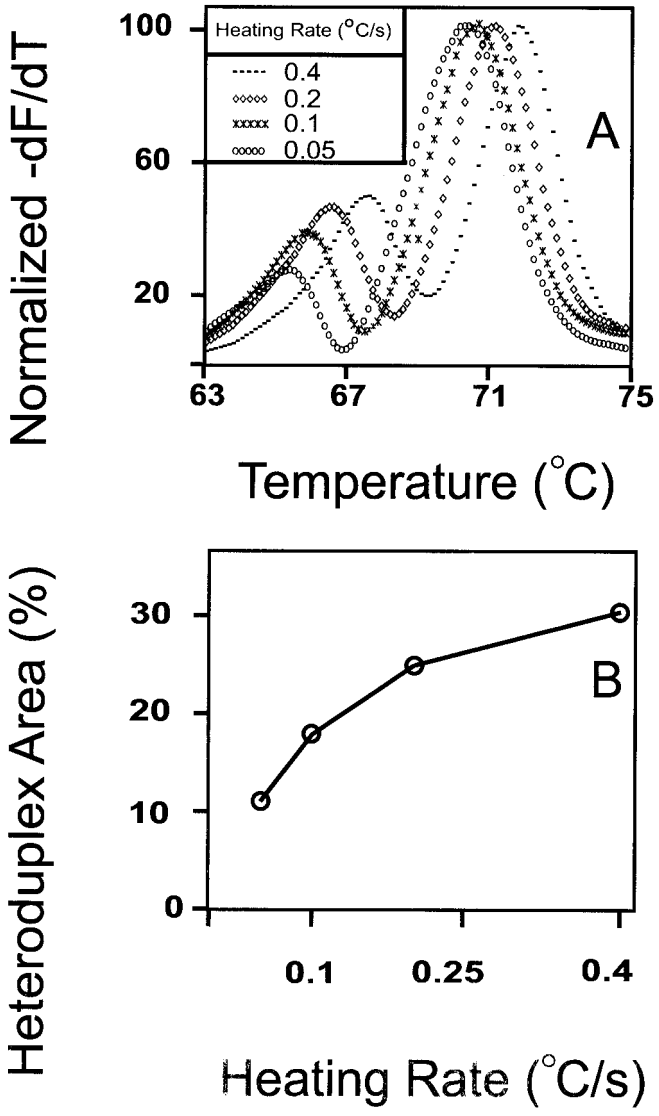

Fig. 3. Heteroduplex melting is more apparent at faster heating rates.

Heterozygous F508del DNA was amplified with one labeled primer as in Fig. 1B. The sample was repeatedly denatured, cooled at a programmed rate of 20 °C/s, and melted at different rates. (*A*), derivative melting curves normalized to the homoduplex peak height. (*B*), heteroduplex peak area (%) plotted against heating rate. The LightCycler was used for melting curve acquisition.

The effect of amplicon size on heteroduplex detection and genotyping is shown in Fig. 4. All three genotypes of the single-nucleotide polymorphism in the *HTR2A* gene, homozygous T, homozygous C, and heterozygous T/C, were amplified using three different amplicon lengths. Differences among genotypes are easily distinguished. Although the differences decrease as the amplicon size increases, melting curve inspection still allows genotyping with an amplicon size of 304 bp. The homozygous C genotype is always more stable than the homozygous T genotype, allowing differentiation between homozygotes if appropriate controls are used. In contrast to the short cystic fibrosis amplicon (Figs. 1–3), separate heteroduplex peaks on derivative melting curve plots are not present. However, the melting transitions from heterozygotes are broader than the transitions from homozygotes, and the curves from heterozygotes cross the less stable homozygote curve at higher temperatures. Melting curve data are often displayed as derivative plots (Fig. 4, A–C), requiring estimation of the curve derivative. With high-resolution data, we prefer simple fluorescence-vs-temperature plots that do not introduce errors associated with smoothing operations (Fig. 4, D–F). Furthermore, although T_m estimates are conveniently found as peaks on derivative plots, peak estimates are not accurate if the melting transition is asymmetric; i.e., the temperature at which one-half of the duplexes are melted does not correlate with the peak on derivative plots that are asymmetric, such as those resulting from the amplification of heterozygous samples. For asymmetric heterozygous samples, T_ms can be determined directly from normalized melting curves as the temperature of the sample at 50% fluorescence.

Melting curve precision and the ability to distinguish different genotypes depends on the temperature and fluorescence resolution of the instrument. Fig. 5 shows the normalized melting curves of two different DNA samples for each of three different β-globin types: wild type (AA), AS, and SC. The 113-bp amplicons were melted four at a time either in the LightCycler (Fig. 5B) or on the high-resolution instrument (Fig. 5C). Although all genotypes could be distinguished on both instruments, significant noise was apparent in the LightCycler data. The noise increased in severity as more samples were melted at the same time in the LightCycler (data not shown).

The normalized melting curves of the four most common β-globin homozygotes are shown in Fig. 6. Three different samples for each genotype were analyzed, except for the rare EE genotype, where only one sample was available. All four genotypes were easily distinguished.

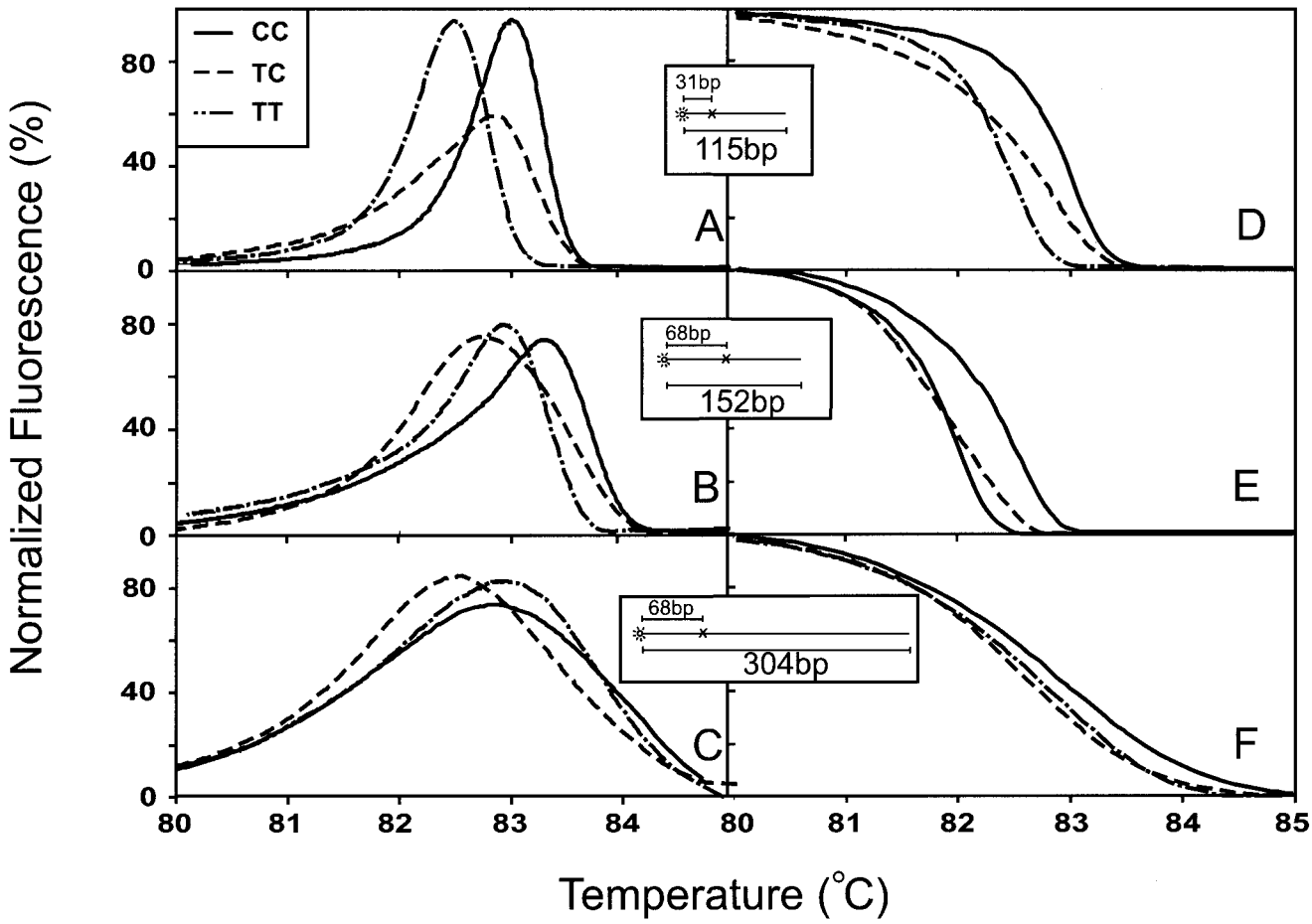

Fig. 4. Genotyping of the T102C polymorphism of *HTR2A* with a labeled primer at three different amplicon lengths: 115 (*A* and *D*), 152 (*B* and *E*), and 304 bp (*C* and *F*).

Both derivative melting curve plots (*A–C*) and normalized melting curves (*D–F*) are shown. The positions of the fluorescent label and polymorphism are shown to scale in each *inset*. In each case, 6-carboxyfluorescein was used as the label. For the longer products (152 and 304 bp), the label was attached to a 5′ G residue, and the fluorescence decreased 8% during melting. For the 115-bp product, the label was attached to a 5′ C residue, and the fluorescence increased 10% during melting (for easy comparison with the longer products, the curves in *A* and *D* are inverted). The high-resolution melting instrument was used for melting curve acquisition.

This is particularly impressive for the AA vs SS types, where the only difference is an A:T base pair that is replaced with a T:A base pair.

The normalized melting curves of the four most common β-globin heterozygotes are shown along with wild-type homozygotes in Fig. 7. Two different samples were analyzed for each genotype. All four heterozygotes (AC, AE, AS, and SC) were clearly distinguished from the wild type, with partial melting before the major wild-type transition. Furthermore, the melting curves of all heterozygotes were different from each other; i.e., not only could the presence of a heterozygote be discerned, but the exact heterozygote could be identified.

Four different β-globin heterozygous AC samples [typed by conventional adjacent hybridization probes *(16)*] and four different wild-type samples were amplified and analyzed by high-resolution melting (data not shown). The wild-type and AC groups were clearly distinct, except for one "AC" sample with a melting curve between the wild-type and AC clusters. Sequencing of the aberrant sample revealed an AC genotype with an additional heterozygous base within the sequence of the labeled primer, TGCA(C/T)CTGACTCCT.

Fig. 8 demonstrates the use of a generic indicator primer for detection of sequence alterations with use of a 243-bp amplicon of the cystic fibrosis gene. The location and identity of the polymorphisms and the orientation of the three primers are shown in Fig. 8A. The normalized melting curves of two homozygotes and four heterozygotes are shown in Fig. 8B. All four heterozygotes showed partial melting well before the major wild-type transition, distinguishing them from the homozygous samples.

Discussion

Double-strand-specific DNA dyes seem like ideal candidates for high-resolution melting analysis of different genotypes. For example, SYBR Green I is a dye extensively used for melting analysis and shows a large change in fluorescence during PCR *(8, 22)*. Conceivably, such

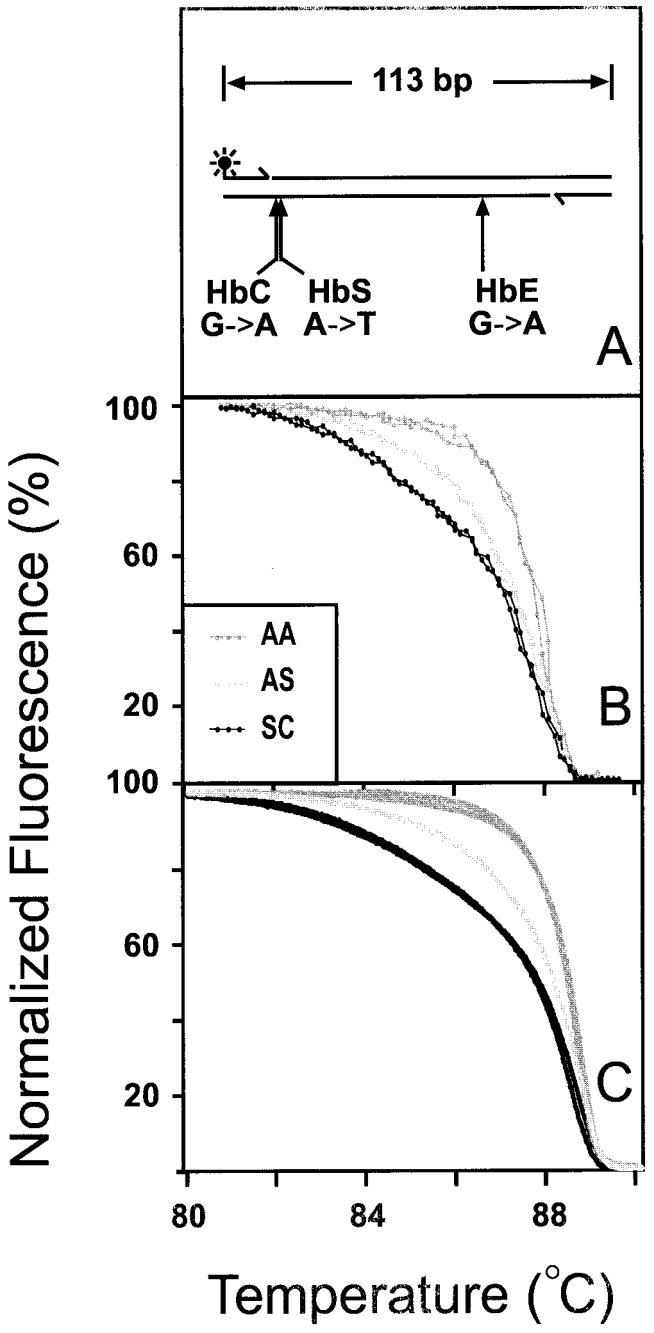

Fig. 5. Comparison of melting curves obtained on two different instruments.

(*A*), scale drawing of the 113-bp β-globin product. Two different samples of each type [wild type (AA), heterozygous sickle cell (AS), and heterozygous SC] were amplified and analyzed. (*B*), melting data acquired on the LightCycler (heating to 95 °C, cooling to 60 °C, and continuous collection of fluorescence at a ramp rate of 0.2 °C/s to 95 °C). Although six curves are shown, the samples were run four at a time, and the data were overlaid for presentation. After the samples were melted in the LightCycler, they were again denatured, cooled, transferred to the high-resolution instrument, and melted at 0.2 °C/s to produce the data shown in *panel C*. In both cases, points indicate actual data acquired. In *panel C*, the data density is high enough that the points appear as smooth lines. The primer was labeled with Oregon Green, using Simple Probe chemistry, to a 5′ T residue, producing a 20% decrease in fluorescence with melting.

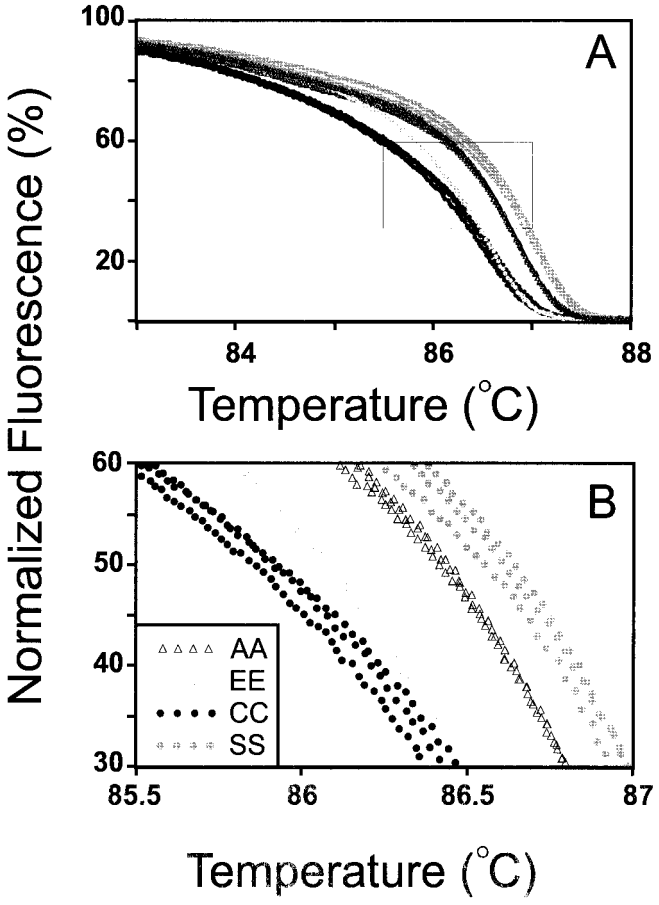

Fig. 6. Melting curve genotyping of homozygous β-globin sequence variants AA, EE, CC, and SS.

Three samples were run for each genotype except for EE, for which only a single sample was available. After amplification, the samples were denatured and cooled in the LightCycler, and then transferred to the high-resolution instrument for melting. Normalized melting curves are shown in *panel A*. The magnified data subset shown in *panel B* clearly displays individual acquisitions and clustering of each genotype. The primer was labeled with Oregon Green to a 5′ T residue, producing an 8% decrease in fluorescence with melting.

dyes could be used for both homozygous genotyping and scanning for heterozygous sequence alterations. SYBR Green I was first used in melting analysis to distinguish PCR products that differed in T_m by ≥2 °C *(9)*. Subsequently, SYBR Green I was used to identify deletions *(23)*, genotype dinucleotide repeats *(24)*, and various sequence alterations *(10, 25–27)*. However, the T_m difference between genotypes can be small and may challenge the resolution of current instruments. Indeed, it has been suggested that SYBR Green I "should not be used for routine genotyping applications" *(28)*. Disadvantages of melting curve genotyping with double-strand-specific DNA dyes include an increased T_m with broadening of the melting transition *(29)* and compression of the T_m difference among genotypes (Fig. 1). These factors lower the potential of SYBR Green I for genotype discrimination.

Amplification of heterozygous DNA produces four different single strands that create two homoduplex and two heteroduplex products when cooled. Theoretically,

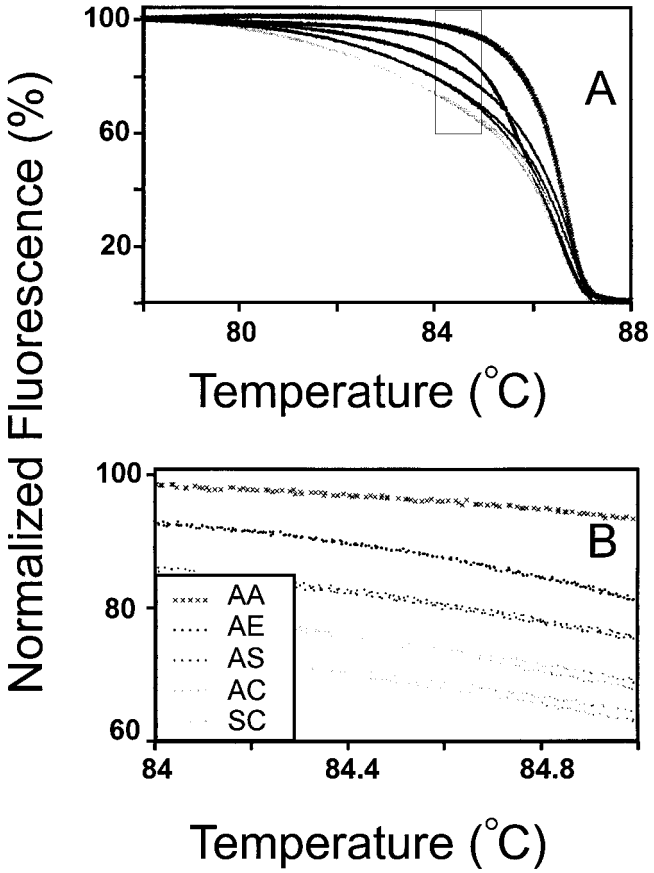

Fig. 7. Melting curve genotyping of heterozygous β-globin sequence variants AE, AS, AC, and SC compared with the wild type (AA).

Samples were run in duplicate. The high-resolution melting instrument was used. The magnified data subset is shown in *panel B*. Primer labeling was as given in the legend for Fig. 5.

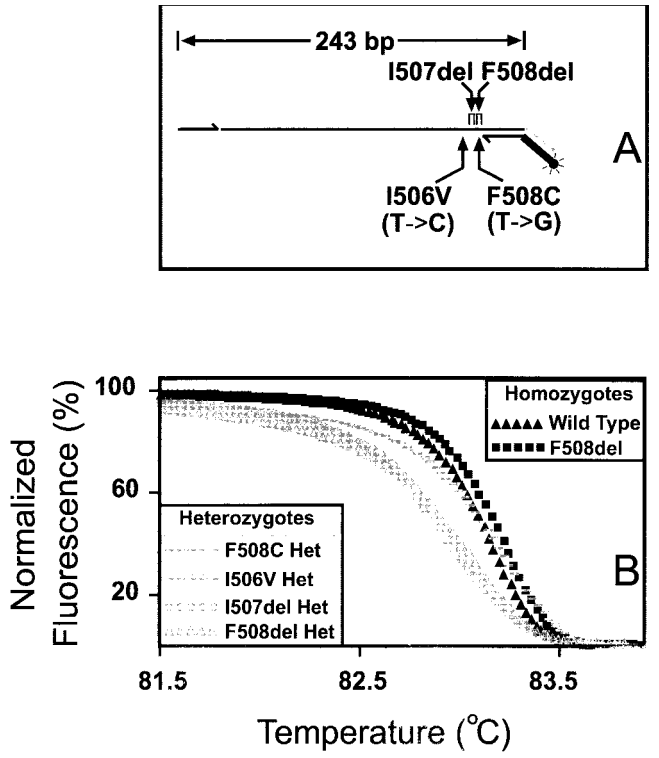

Fig. 8. Genotyping with a labeled generic indicator primer.

A 243-bp fragment of the cystic fibrosis gene was amplified in the presence of three primers (*A*): a generic indicator primer (reverse primer; *thick line*), an unlabeled primer with a 5′-tail identical in sequence (without the 5′ G) to the indicator (reverse primer; *thin line* plus *thick line*), and an opposing, unlabeled primer (forward primer; *thin line*). Multiple rounds of PCR incorporate the indicator primer into the major PCR product. Melting curves resulting from wild-type DNA, two 3-base deletions (F508del and I507del), and two single-nucleotide polymorphisms (F508C and I506V) are shown in *panel B*. The indicator primer was labeled with 6-carboxyfluorescein to a 5′ G residue, producing a 20% decrease in fluorescence with melting.

all four products have different T_ms, and the melting curve should be a composite of all these transitions. However, double-strand-specific DNA dyes may redistribute during melting *(30)*, causing release of the dye from low-melting heteroduplexes and redistribution to higher-melting homoduplexes. Because SYBR Green I is not saturating at concentrations compatible with PCR *(8)*, such redistribution is plausible and consistent with the absence of a heteroduplex transition (Fig. 1C).

The use of labeled primers for melting analysis avoids the majority of problems associated with SYBR Green I. There is no dye to redistribute, no increase in amplicon T_m, no broadening of the melting transition, and no T_m compression among genotypes. In contrast to SYBR Green I, a heteroduplex transition occurs when amplicons with labeled primers are melted (Fig. 1B). However, strand reassociation is still possible with labeled primers; i.e., heteroduplex strands may reassociate with their perfect complement and form homoduplexes during melting. Because the concentration of products at the end of PCR is high, this reassociation happens rapidly. Reassociation can be minimized by limiting the time the products are near their T_ms, particularly between the T_ms of the heteroduplex and homoduplex products. Fast heating rates (Fig. 3) and low Mg^{2+} concentrations limit strand reassociation. Increased ionic strength and, particularly, divalent cations are known to increase duplex reassociation rates *(31)*. Practical limitations to rapid heating include difficulty with maintaining temperature homogeneity within samples, fewer fluorescence acquisitions per temperature interval, and broadening of the transition from non-equilibrium effects.

In addition to strand reassociation during melting, the selective hybridization of a strand to either its perfect match or to its mismatched complementary strand is influenced by cooling rates and ionic strength. Under our conditions, heteroduplex formation is most favored by rapid cooling and disappears at rates <0.1 °C (Fig. 2). This is in contrast to denaturing HPLC methods, where cooling rates are much slower (0.01–0.02 °C/s) but heteroduplexes are formed efficiently *(7)*. Perhaps the relative rates of homoduplex and heteroduplex formation are strongly dependent on product size, and our results using small amplicons are not typical for the larger products more

commonly used in denaturing HPLC. The effect of cooling rate and ionic strength on the competitive formation of single-strand conformers, heteroduplexes, and homoduplexes deserves further systematic study.

Various fluorescent dyes can be used to label the primers. Single-labeled oligonucleotides are attractive for their simplicity *(12, 14)*. Most dyes attached to oligonucleotides change fluorescence when the oligonucleotide hybridizes. Oregon Green 488, 6-carboxyfluorescein, and BODIPY-FL all work with most sequences and conveniently use the common SYBR Green I/fluorescein fluorescence channel. Cy5 and Texas Red also work well but require special excitation and emission wavelengths.

The effect of sequence on the fluorescence change with hybridization is complex *(32)* and will require further study. However, some tentative generalizations can be made. The magnitude of the fluorescence change with amplicon melting varied from 8% to 20% (see figure legends). In all but one case (115-bp *HTR2A*), the fluorescence decreased with melting (increased with hybridization). In the case of the exception, 6-carboxyfluorescein was attached to a C residue, and the results are consistent with deoxyguanosine quenching as reported previously *(14)*. However, when 6-carboxyfluorescein or Oregon Green was attached to a G residue in the primer (cystic fibrosis targets and the longer *HTR2A* targets), the fluorescence decreased with melting. The mechanism for this is not known, but it is consistent with inherent G quenching in the primer decreasing with hybridization. When Oregon Green was attached to a T residue, the fluorescence also decreased with melting (β-globin targets). This effect was enhanced through SimpleProbe attachment (a proprietary linking chemistry) and further augmented by a high pH and ionic strength. However, these modifications are not generally necessary. Indeed, one of the greatest changes in fluorescence was obtained when we used direct attachment of 6-carboxyfluorescein to two G residues in the indicator primer (Fig. 8). Furthermore, the temperature and fluorescence resolution of the instrument appears more important than the absolute fluorescent change that occurs with melting. No special primer selection criteria were used.

All homozygotes tested at the *HTR2A*, β-globin, and cystic fibrosis loci were distinguishable by T_m on the high-resolution instrument. In each case, the order of duplex stability matched theoretical predictions *(22)*. Four of six possible single-nucleotide polymorphisms were included in this study (A/T, C/T, G/T, and G/A), and even the A/T alteration of Hb SS was distinguishable from the wild type (Fig. 6). Further studies will be necessary to define the limits of homozygote differentiation with this technique. The missing G/C and C/A polymorphisms need to be tested, as well as the effect of amplicon length and distance from the labeled primer to the polymorphism.

As the amplicon size increases, the difference between genotypes decreases (Fig. 4). The discrimination between homozygous genotypes can be improved by melting at slower rates, at the expense of longer analysis time. The instrument resolution is also important (Fig. 5) in genotype discrimination. The LightCycler uses a 12-bit temperature converter that limits the temperature resolution to 8–9 divisions per 1 °C. In addition, the number of acquisitions per 1 °C depends on the number of samples in the LightCycler. Nevertheless, the LightCycler can be used for genotyping of the targets studied in this report when only a few samples are monitored. LightCycler melting curve data are best exported in spreadsheet format and processed by normalization as described in the *Materials and Methods*. Derivative plots of LightCycler data are not recommended because the noise present can produce misleading artifacts when the derivative is taken. The high-resolution instrument uses 16-bit data conversion of both temperature and fluorescence. The high-resolution instrument also ensures greater temperature homogeneity within each sample because the capillary is completely surrounded by a solid aluminum cylinder.

One source of potential error in melting curve genotyping is the effect of DNA concentration on T_m. When a random 100-bp amplicon of 50% GC content was used under PCR conditions, the difference in T_m between products at 0.05 μM and 0.5 μM was ~0.7 °C *(21, 33)*. This change can be important when the T_ms of different homozygous genotypes are very close. However, different PCR samples tend to plateau at the same product concentration, so concentration differences will usually be minimal. It may also be possible to estimate amplicon concentrations by real-time fluorescence and adjust the T_ms for even greater genotyping precision.

Whatever the precision of the instrument, some genotypes will be nearly identical in T_m. One way to detect homozygous variants with the same T_m is to mix the variants together. The resulting heteroduplexes will melt at lower temperatures than the homoduplexes, displayed as a drop in the normalized melting curves before the major melting transition (Figs. 4, 5, 7, and 8).

Different heterozygotes are distinguishable (Fig. 7) because the shapes of the melting curves are defined by the stabilities and/or kinetic melting rates of the two heteroduplexes and the two homoduplexes present. Hb SC has a longer low-temperature shoulder than do other heterozygotes (Figs. 5 and 7) because the SC heteroduplexes are mismatched in two adjacent positions. Heteroduplexes from single-nucleotide polymorphisms (AS, AC, and AE) are all mismatched in only one position, but they display different melting curves because different mismatches are present in the heteroduplexes and/or their positions in the amplicon are different. The single-base heterozygotes studied here include three of four possibilities (A/T:T/A, A/C:T/G, and T/C:A/G). Although the G/C:C/G combination was not studied, the A/T:T/A combination is reported to be the most difficult to detect on heteroduplex analysis *(3)*.

For heterozygote detection, the absolute T_m and the

influence of DNA concentration are not as important as the shape of the curve, particularly at the "early", low-temperature portion of the transition. Unexpected sequence variants in one allele are generally expected to produce more low-temperature melting. An interesting exception is the unexpected variant under the β-globin primer that reduced low-temperature melting in a known AC heterozygote. This is consistent with both sequence alterations being in *cis*, leading to allele-specific amplification of the AA amplicon. Fewer heteroduplexes in this sample produced a melting curve between the AA and AC clusters.

This report has focused on using labeled primers and amplicon melting analysis to detect and genotype known sequence variants. The sensitivity of this method for detecting unknown sequence variants (mutation scanning) remains to be studied in detail. The three targets reported here (cystic fibrosis, β-globin, and *HTR2A*) were the first three attempted. Targets up to 303 bp in length (*HTR2A*) with mutations up to 75 bases away from the fluorescent label (Hb E) were genotyped. However, the fourth target we attempted was apolipoprotein E. A 181-bp amplicon was designed to bracket the e3/e4 and e3/e2 polymorphisms. Only the polymorphism closest to the labeled primer could be genotyped, indicating that sequence alterations far enough away from the label (in the apolipoprotein E case, 160 bp) may go undetected. One possible solution is to label both primers, preferably with different dyes that have spectrally distinct emissions. Color multiplexing techniques *(12)* can be used to follow the melting of both labels, monitoring both sides of the amplicon. Detection might still fail if the sequence variation is in an internal domain that melts before or after both ends.

Equilibrium domain melting theory *(34)* may or may not apply to rapid melting rates of 0.1–0.4 °C/s. Unlike denaturing gradient gel electrophoresis, the informative domain is not the first melting domain but should be the domain that includes the labeled primer. If the sequence variation is outside of the domain that contains the labeled primer, one might expect it to be missed. However, it is not easy to predict melting domains when a mismatch is present. Conventional melting maps for the completely homologous targets studied here are provided in the online supplement. It does not appear that the sequence alterations need to be in the same domain as the labeled primer to be detected.

In contrast to melting domain theory, nearest-neighbor, "all or none" T_m estimates can account for single-base mismatches *(21)*. The predicted and observed T_ms for the genotypes studied are presented in the data supplement that accompanies the online version of this article at http://www.clinchem.org/content/vol49/issue3/. Parameters are not available for 3-bp deletions (cystic fibrosis) and adjacent mismatches (Hb CS). When the melting transition is not symmetric (as in all heterozygous genotypes), the observed T_m is taken as the temperature where 50% of the duplex is melted, not as the peak from derivative plots. The predicted and observed T_m differences between the wild type and mutant (ΔT_m) for homozygotes are also provided in the online supplement. Observed ΔT_ms for heterozygotes can be measured only if the homoduplex and heteroduplex transitions are distinct. With our targets, this is possible only with the short cystic fibrosis amplicon, and even with this target, the grouping of homoduplex and heteroduplex transitions into peaks may not be correct. Melting curves of products that result from amplification of heterozygotes overlay the melting curves of four distinct duplexes. In general, four distinct T_ms cannot be extracted from these data, and the composite "T_m " is not as useful as the complete normalized melting curve. For example, the different heterozygotes in Fig. 7 have very similar T_ms, but they are distinctly different in the low-temperature melting region.

Because no internal probes are used, the quality of melting analysis with labeled primers depends on the quality of the PCR. Surprisingly, the method is more robust than might be expected. For example, the DNA for β-globin typing was extracted from blood spots on filter paper and was not highly purified or quantified before analysis. Two different enzymes and buffer systems were used to amplify the β-globin target (Figs. 5–7). The PCR for Fig. 7 was cleaner (less undesired, alternative products) than the PCR for Fig. 6, as evidenced by a more horizontal melting curve at low temperatures before the major transition. Nevertheless, the curves in Fig. 6 still allow unambiguous genotyping; i.e., any "nonspecific" amplification tends to be equal across genotypes and can often be separated from the relevant melting curve differences among genotypes. Still, "hot start" techniques that reduce undesired amplification products may improve differentiation.

Amplicon melting with labeled primers has distinct advantages over current techniques for genotyping and mutation scanning. This method is a closed-tube system and requires no sample processing after the beginning of PCR. A melting curve acquired at 0.3 °C/s requires ~1 min. The ability to use a generic indicator primer means that only one fluorescently labeled oligonucleotide needs to be synthesized to analyze many targets. One primer for each target is modified to include a 5′ tail of the indicator sequence. Multiple rounds of PCR incorporate the labeled primer into the final amplicon. Reactions require three oligonucleotides instead of two, but the same fluorescently labeled oligonucleotide can be used, in theory, for all targets. Further study will delineate the usefulness and limits of labeled primers in genotyping and mutation scanning.

This work was funded by NIH (Grants GM58983 and GM60063), Idaho Technology, and the University of Utah. We thank Dr. Philip Bernard for the development and concept of the high-resolution instrument (GM60063). We

thank Rich Abbott and Derek David for initial work on the high-resolution instrument prototype and Idaho Technology for providing the HR-1 instrument. We also thank Steve Dobrowolski for providing the different hemoglobin genotypes as blood spots on filter paper. The LightCycler instrument and related techniques are licensed by the University of Utah to Idaho Technology and from Idaho Technology to Roche Applied Systems. C.T.W. holds equity interest in Idaho Technology.

References

1. Lyon E, Millson A, Phan T, Wittwer CT. Detection of base alterations within the region of factor V Leiden by fluorescent melting curves. Mol Diagn 1998;3:203–10.
2. Orita O, Iwahana H, Danazawa J, Hayashi K, Sekiya T. Detection of polymorphisms of human DNA by gel electrophoresis as single-strand conformation polymorphisms. Proc Natl Acad Sci U S A 1989;86:2766–70.
3. Nataraj AJ, Olivos-Glander I, Kusukawa N, Highsmith WE. Single-strand conformation polymorphism and heteroduplex analysis for gel-based mutation detection. Electrophoresis 1999;20:1177–85.
4. Abrams ES, Murdaugh SE, Lerman LS. Comprehensive detection of single base changes in human genomic DNA using denaturing gradient gel electrophoresis and a GC clamp. Genomics 1990;7:463–75.
5. Wartell RM, Hosseini S, Powell S, Zhu J. Detecting single base substitutions, mismatches and bulges in DNA by temperature gradient gel electrophoresis and related methods. J Chromatogr A 1998;806:169–85.
6. Taylor GR, Deeble J. Enzymatic methods for mutation scanning. Genet Anal 1999;14:181–6.
7. Xiao W, Oefner PJ. Denaturing high-performance liquid chromatography: a review. Hum Mutat 2001;17:439–74.
8. Wittwer CT, Herrmann MG, Moss AA, Rasmussen RP. Continuous fluorescence monitoring of rapid cycle DNA amplification. Biotechniques 1997;22:130–1,134–8.
9. Ririe KM, Rasmussen RP, Wittwer CT. Product differentiation by analysis of DNA melting curves during the polymerase chain reaction. Anal. Biochem 1997;245:154–60.
10. Lipsky RH, Mazzanti CM, Rudolph JG, Xu K, Vyas G, Bozak D, et al. DNA melting analysis for detection of single nucleotide polymorphisms. Clin Chem 2001;47:635–44.
11. Elenitoba-Johnson KSJ, Bohling SD. Solution-based scanning for single-base alterations using a double-stranded DNA binding dye and fluorescence-melting profiles. Am J Pathol 2001;159:845–53.
12. Wittwer CT, Herrmann MG, Gundry CN, Elenitoba-Johnson KSJ. Real-time multiplex PCR assays. Methods 2001;25:430–42.
13. Millward H., Samowitz W., Wittwer CT, Bernard PS. Homogeneous amplification and mutation scanning of the p53 gene using fluorescent hybridization probes, Clin Chem 2002;48:1321–8.
14. Crockett AO, Wittwer CT. Fluorescein-labeled oligonucleotides for real-time PCR: using the inherent quenching of deoxyguanosine nucleotides. Anal Biochem 2001;290:89–97.
15. Gundry CN, Bernard PS, Herrmann MG, Reed GH, Wittwer CT. Rapid F508del and F508C assay using fluorescent hybridization probes. Genet Test 1999;3:365–70.
16. Herrmann M, Dobrowolski S, Wittwer CT. β-Globin genotyping by multiplexing probe melting temperature and color. Clin Chem 2000;46:425–8.
17. Heath E, O'Brien D, Banas R, Dobrowolski SF. Optimization of an automated protocol to isolate DNA from Guthrie cards. Arch Pathol Lab Med 1999;123:1154–60.
18. Wittwer CT, Ririe KM, Andrew RV, David DA, Gundry RA, Balis UJ. The LightCycler™: a microvolume, multisample fluorimeter with rapid temperature control. Biotechniques 1997;22:176–81.
19. Savitzky-Golay smoothing filters. In: Press WH, Teukolsky SA, Vetterling WT, Flannery BP, eds. Numerical recipes in C, 2nd ed. New York: Cambridge University Press, 1992:650–5.
20. Nuovo GJ, Hohman RJ, Nardone GA, Nazarenko IA. In situ amplification using universal energy transfer-labeled primers. J Histochem Cytochem 1999;47:273–9.
21. von Ahsen N, Wittwer CT, Schutz E. Oligonucleotide melting temperatures under PCR conditions: nearest-neighbor corrections for Mg^{2+}, deoxynucleotide triphosphate, and dimethyl sulfoxide concentrations with comparison to alternative empirical formulas. Clin Chem 2001;47:1956–61.
22. Wittwer CT, Kusukawa N. Real-Time PCR. In: Persing D, Tenover F, Relman D, White T, Tang Y, Versalovic J, Unger B, eds. Diagnostic molecular microbiology: principles and applications. Washington, DC: ASM Press, 2003:in press.
23. Aoshima T, Sekido Y, Miyazaki T, Kajita M, Mimura S, Watanabe K, et al. Rapid detection of deletion mutations in inherited metabolic diseases by melting curve analysis with LightCycler. Clin Chem 2000;46:119–22.
24. Marziliano N, Pelo E, Minuti B, Passerini I, Torricelli F, Da Prato L. Melting temperature assay for a *UGT1A* gene variant in Gilbert syndrome. Clin Chem 2000;46:423–5.
25. Pirulli D, Boniotto M, Puzzer D, Spano A, Amoroso A, Crovella S. Flexibility of melting temperature assay for rapid detection of insertions, deletions, and single-point mutations of the *AGXT* gene responsible for type 1 primary hyperoxaluria. Clin Chem 2000;46:1842–4.
26. Tanriverdi S, Tanyeli A, Baslamisli F, Koksal F, Kilinc Y, Feng X, et al. Detection and genotyping of oocysts of *Cryptosporidium parvum* by real-time PCR and melting curve analysis. J Clin Microbiol 2002;40:3237–44.
27. Hladnik U, Braida L, Boniotto M, Pirulli D, Gerin F, Amoroso A, et al. Single-tube genotyping of MBL-2 polymorphisms using melting temperature analysis. Clin Exp Med 2002;2:105–8.
28. von Ahsen N, Oellerich M, Schutz E. Limitations of genotyping based on amplicon melting temperature [Letter]. Clin Chem 2001;47:1331–2.
29. Douthart RJ, Burnett JP, Beasley FW, Frank BH. Binding of ethidium bromide to double-stranded ribonucleic acid. Biochemistry 1973;12:214–20.
30. Aktipis S, Martz WW, Kindelis A. Thermal denaturation of the DNA-ethidium complex. Redistribution of the intercalated dye during melting. Biochemistry 1975;14:326–31.
31. Britten RJ, Davidson EH. Hybridization strategy. In: Hames BD, Higgins SJ, eds. Nucleic acid hybridization, a practical approach. Washington DC: IRL Press, 1985:1–15.
32. Nazarenko I, Pires R, Lowe B, Obaidy M, Rashtchian A. Effect of primary and secondary structure of oligodeoxyribonucleotides on the fluorescent properties of conjugated dyes. Nucleic Acids Res 2002;30:2089–95.
33. Wetmur JG. DNA probes: applications of the principles of nucleic acid hybridization. Crit Rev Biochem Mol Biol 1991;26:227–59.
34. Myers RM, Maniatis T, Lerman, LS. Detection and localization of single base changes by denaturing gradient electrophoresis. Methods Enzymol 1987;155:501–27.